GRAN SASSO SCIENCE INSTITUTE

The TeV gamma-ray population of the Milky-Way

the contribution of H.E.S.S. unresolved sources to VHE diffuse emission

Presented by: Vittoria Vecchiotti

Based on a work done in collaboration with: M. Cataldo, G. Pagliaroli, F. L. Villante

The TeV gamma-ray luminosity of the Milky-Way: and the contribution of H.E.S.S. unresolved sources to VHE diffuse emission

https://inspirehep.net/literature/1799863

- Population study of the H.E.S.S. Galactic Plane Survey in order to estimate the **total luminosity of the Milky-Way** and **total source flux** and the contribution of H.E.S.S. **unresolved sources** to VHE diffuse emission;

- **Fading-sources interpretation**: In the hypothesis that the signal is dominated by pulsar-powered sources (TeV-Halos, PWNe) we inferred general properties of the pulsar population.

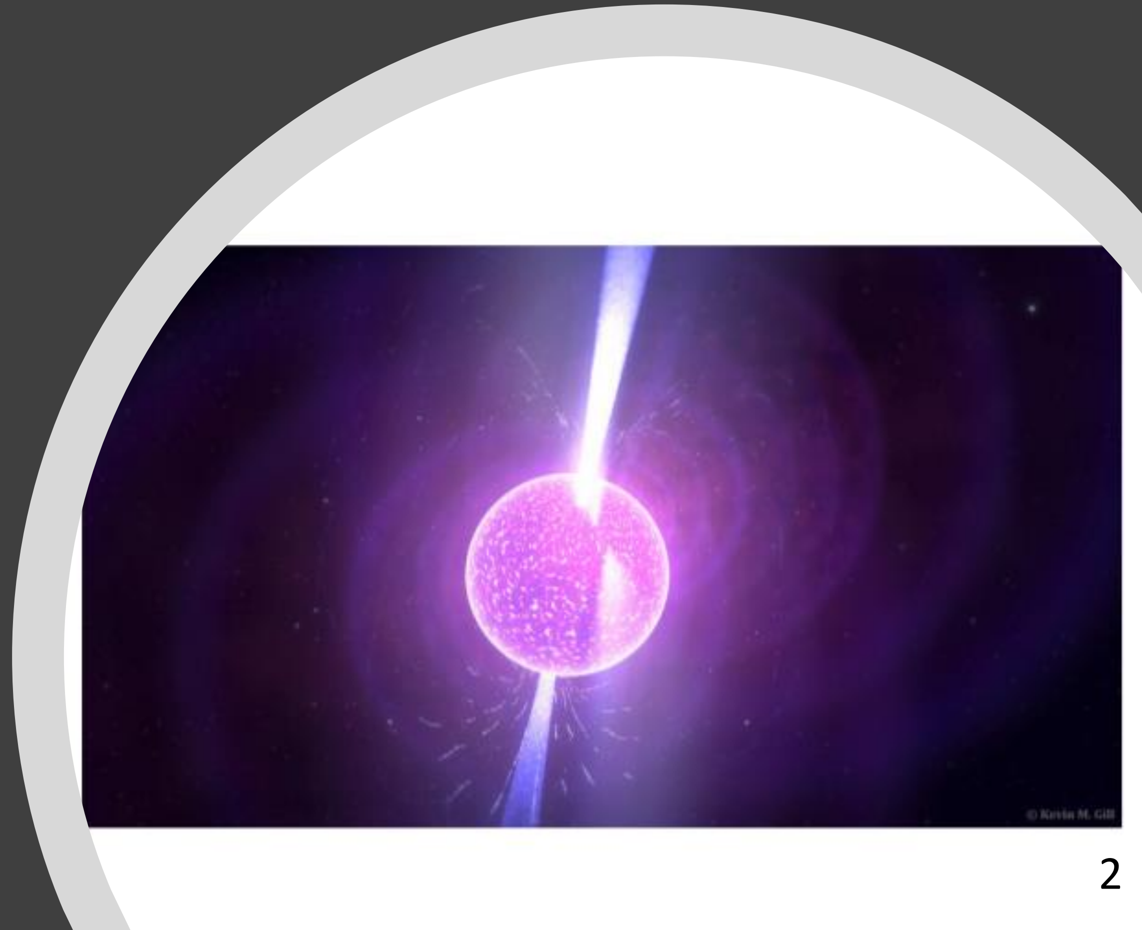

H.E.S.S.:

H.E.S.S. provides observation of the γ-ray sky in the window: $-110^{\circ} < l < 60^{\circ}$ and $|b| < 3^{\circ}$ above 1 TeV.

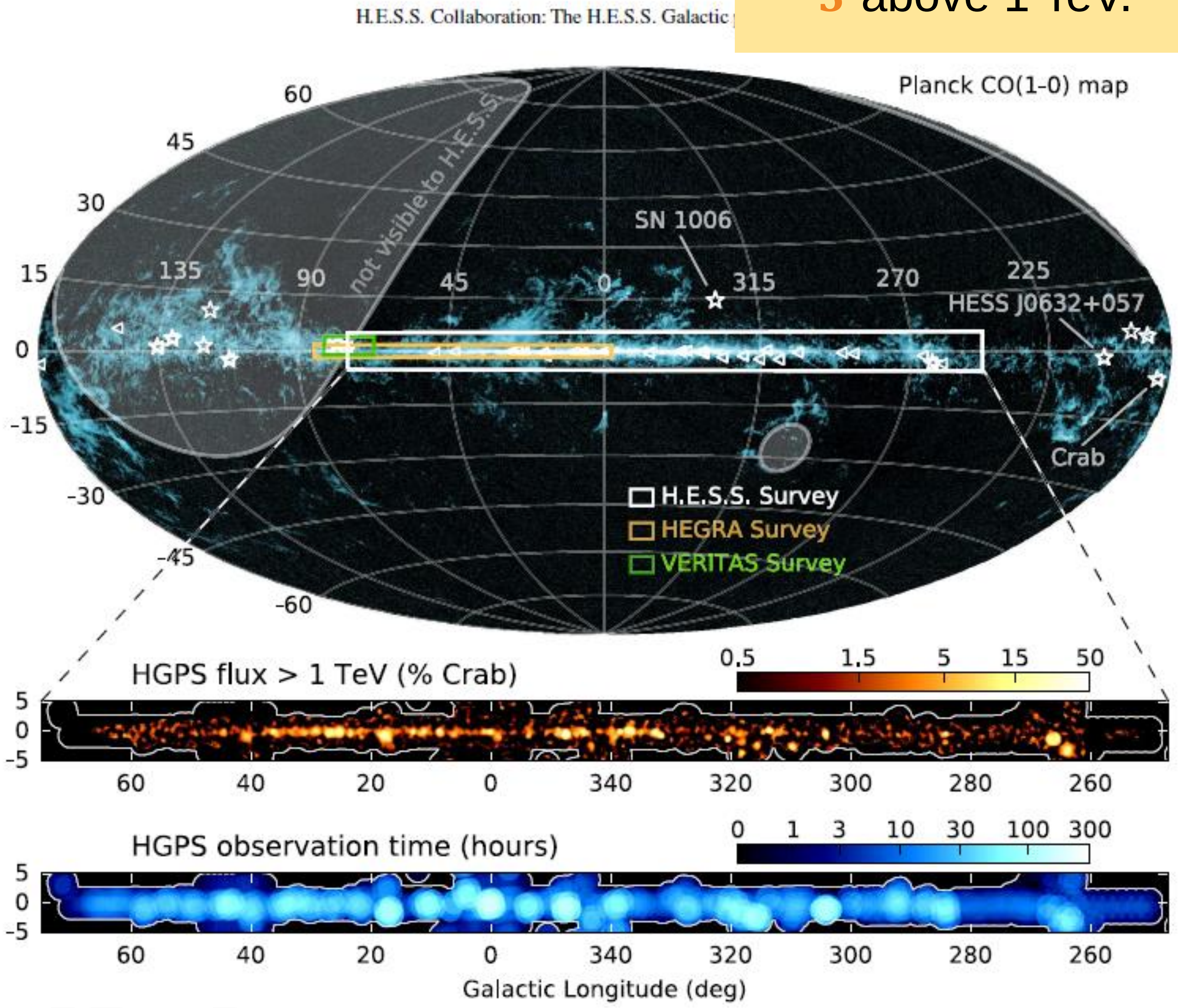

H.E.S.S. sensitivity detection limit:

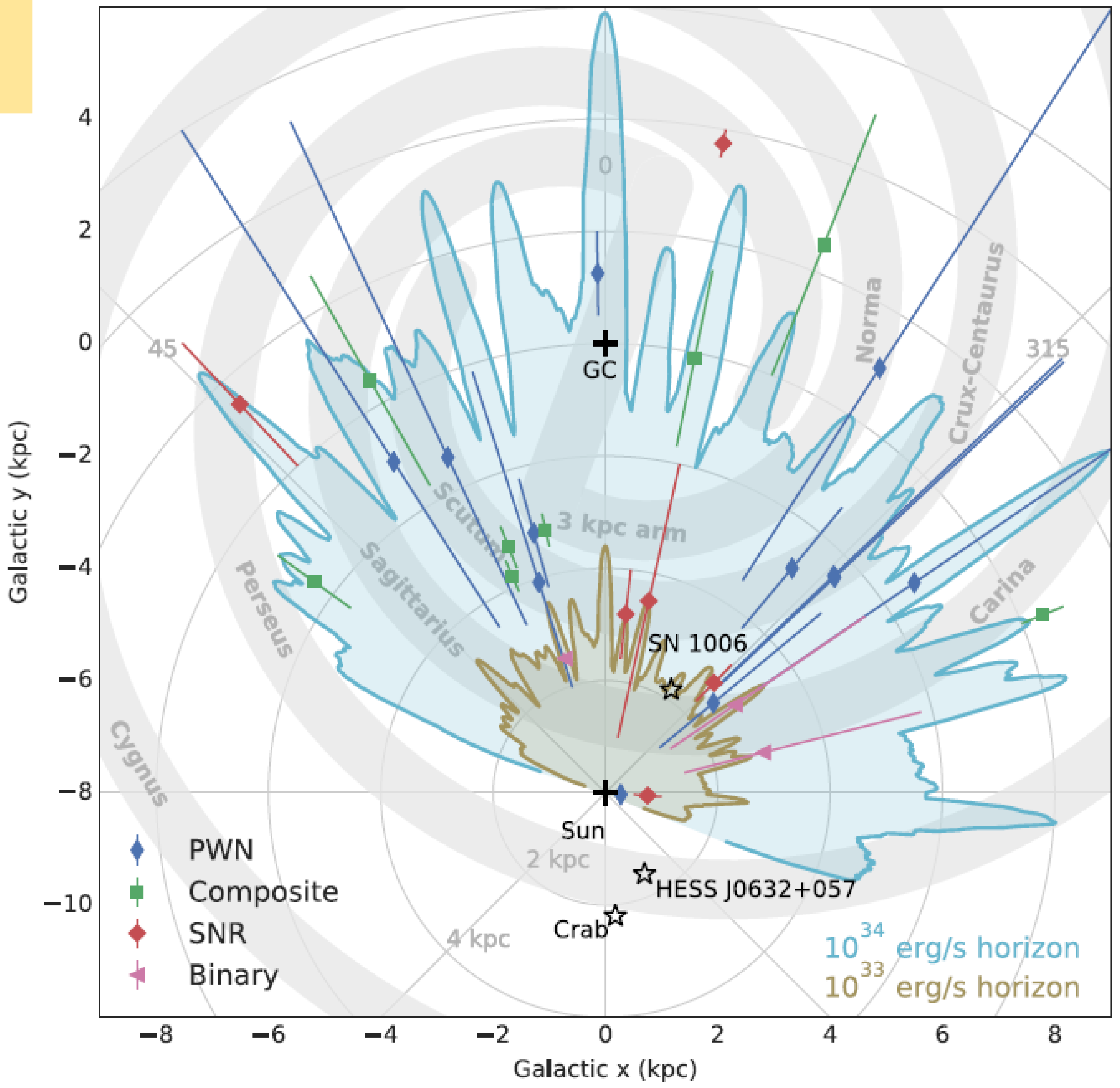

Concerning point-like sources, H.E.S.S. probes a small fraction of the Galaxy up to a median distance of 7.3 kpc for bright ($10^{34}\ erg\ s^{-1}$) sources.

Unresolved sources that contribute to the total diffuse signal.

H.G.P.S catalogue:

- It includes **78 VHE** sources in the H.E.S.S. observational window;
- It provides the integrated flux above 1 TeV of each sources ϕ.

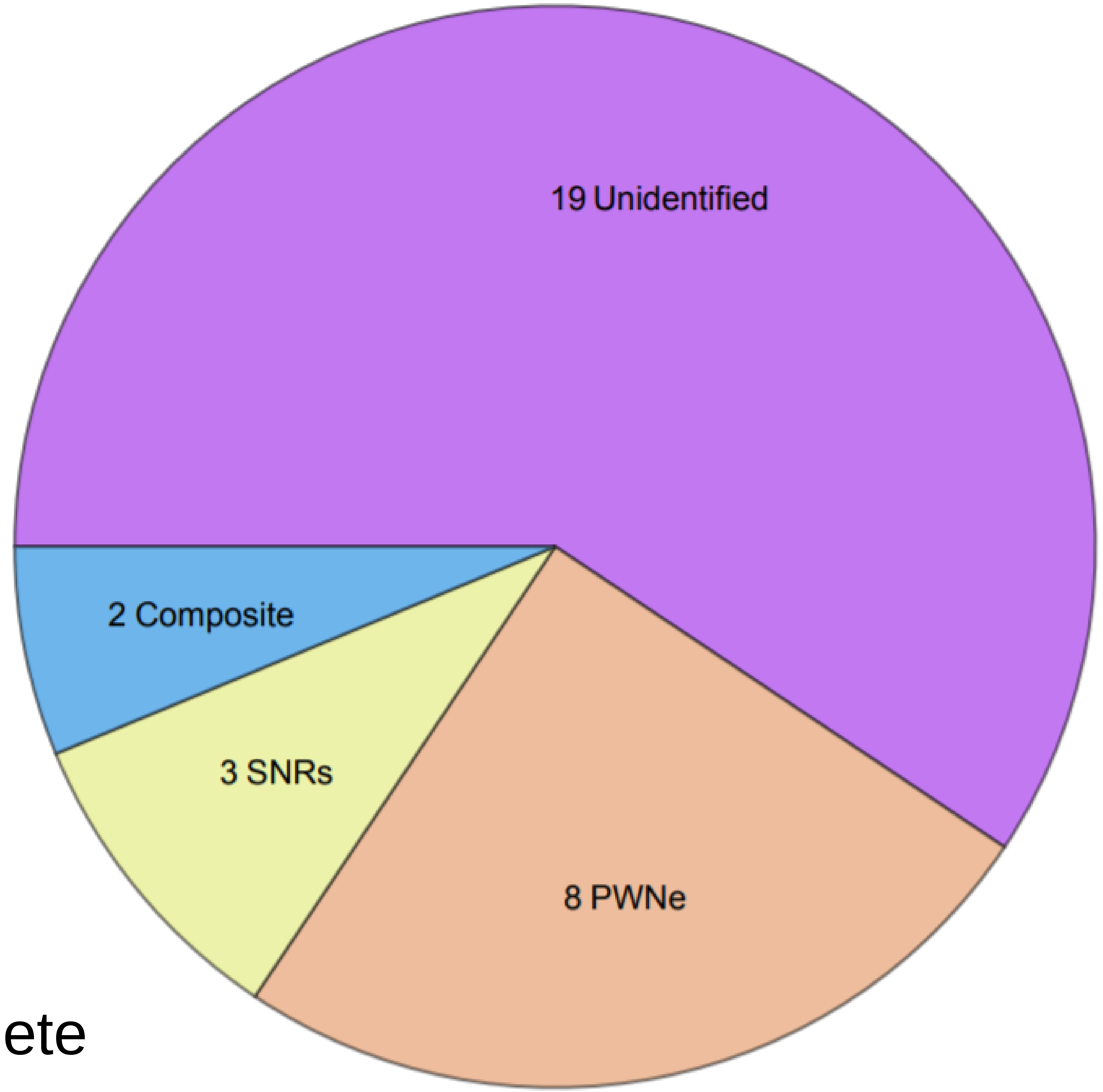

We focus on the brightest sources with flux:

$$\phi > 0.1\phi_{Crab} = 0.1\,(2.26 \times 10^{-11} cm^{-2} s^{-1})$$

The catalogue above this threshold is considered complete (no unresolved sources): **32 sources**.

We assumed a **power-law** energy spectrum with index $\boldsymbol{\beta = 2.3}$ that is the average index of the catalogue for all the sources ;

Model: We postulate the spatial and intrinsic luminosity distribution of the TeV sources:

$$\frac{dN}{dr^3 dL} = \rho(r) Y(L)$$

- The spatial distribution of sources in the Galaxy is assumed to be proportional to the pulsar distribution as in Lormier et Al (2006).;
- The luminosity distribution of sources in the Galaxy is assumed to be a power law:

$$Y(L) = \frac{N}{L_{max}} \left(\frac{L}{L_{max}} \right)^{-\alpha}$$

Reference case:
$\alpha = 1.5$

We have two free parameters:

- the normalization $\boldsymbol{N}$ number of high-luminosity sources
- the maximum luminosity of the population $\boldsymbol{L_{max}}$

Goal: Estimation of the free parameters of our model by fitting H.E.S.S. observational results with an unbinned likelihood

GS
SI

Results:

Best fit values for the reference case:

$$L_{\max} = 4.9^{+3.0}_{-2.1} \times 10^{35} \text{ergs/s}$$
$$\mathcal{N} = 17^{+14}_{-6}$$

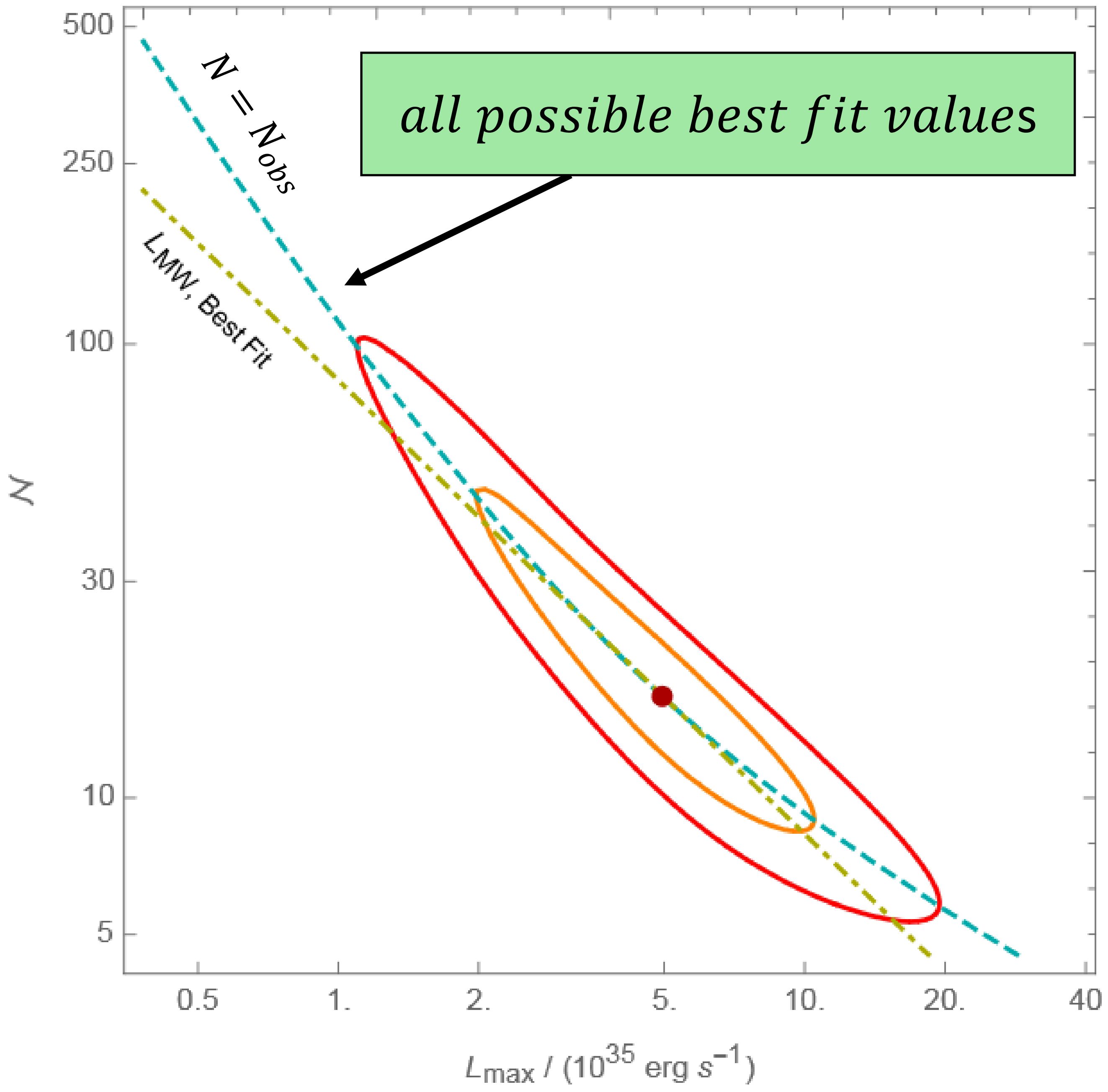

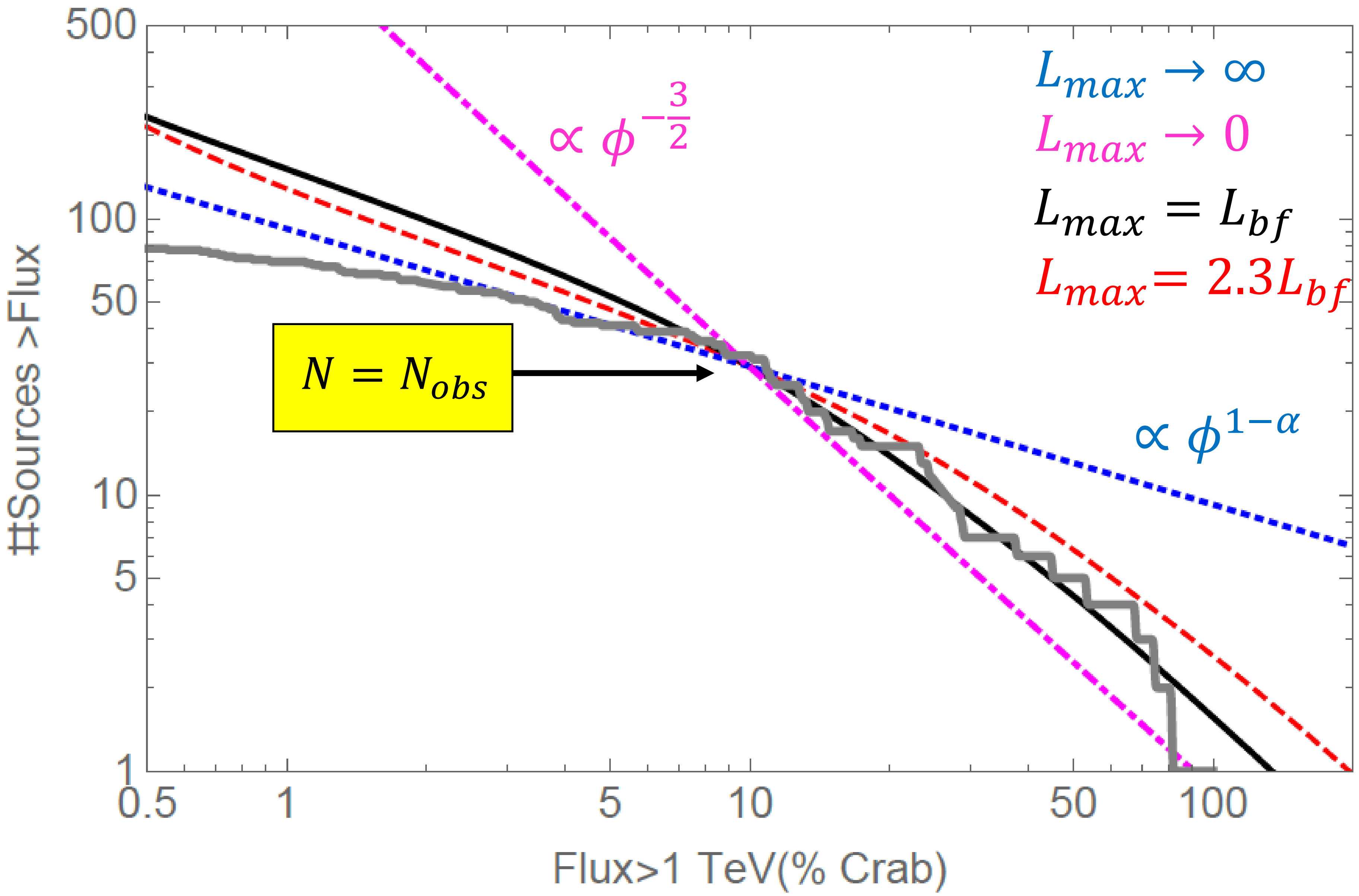

Results:

Best fit values for the reference case:

$$L_{\rm max} = 4.9^{+3.0}_{-2.1} \times 10^{35} {\rm ergs/s}$$
$$\mathcal{N} = 17^{+14}_{-6}$$

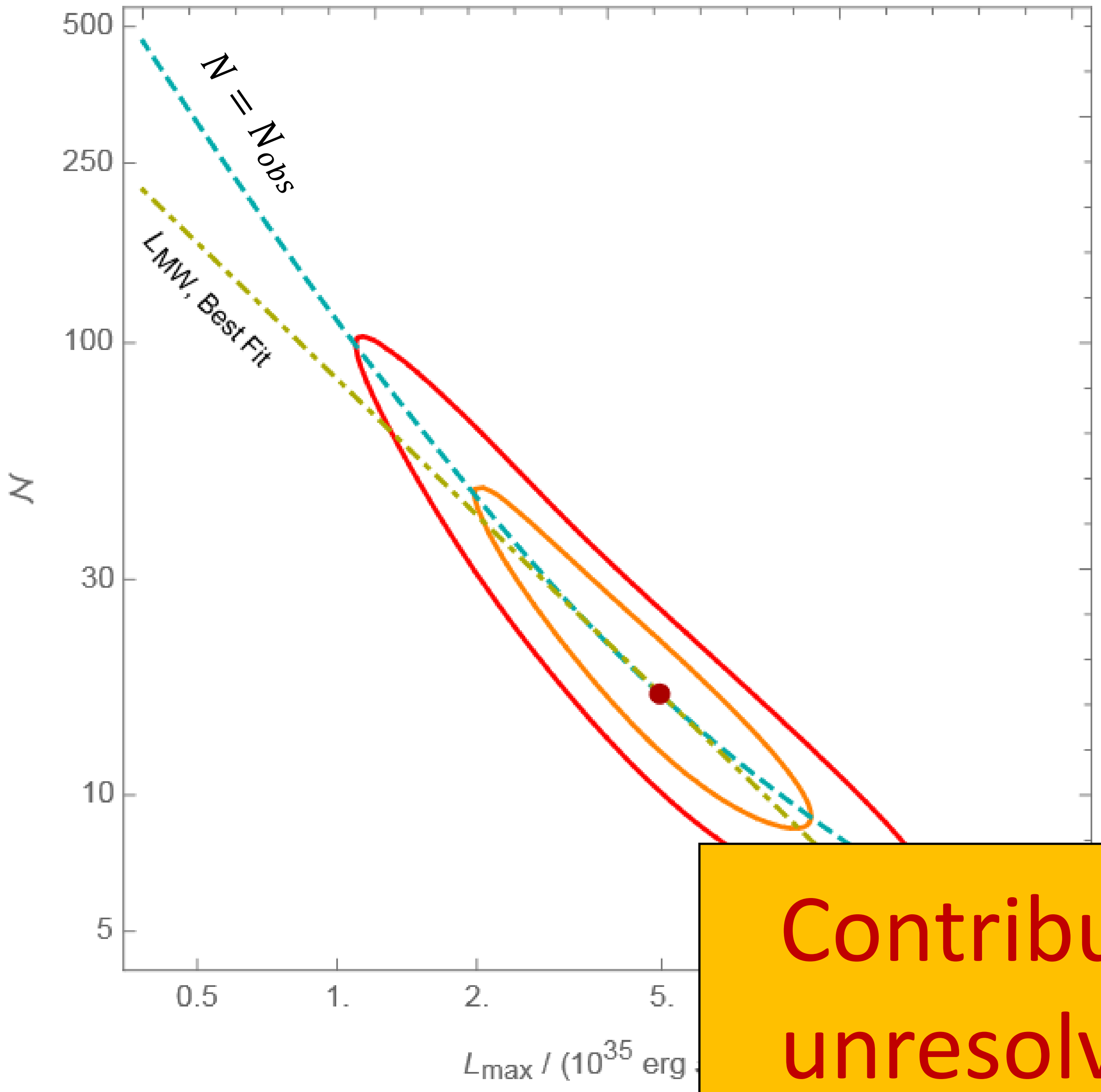

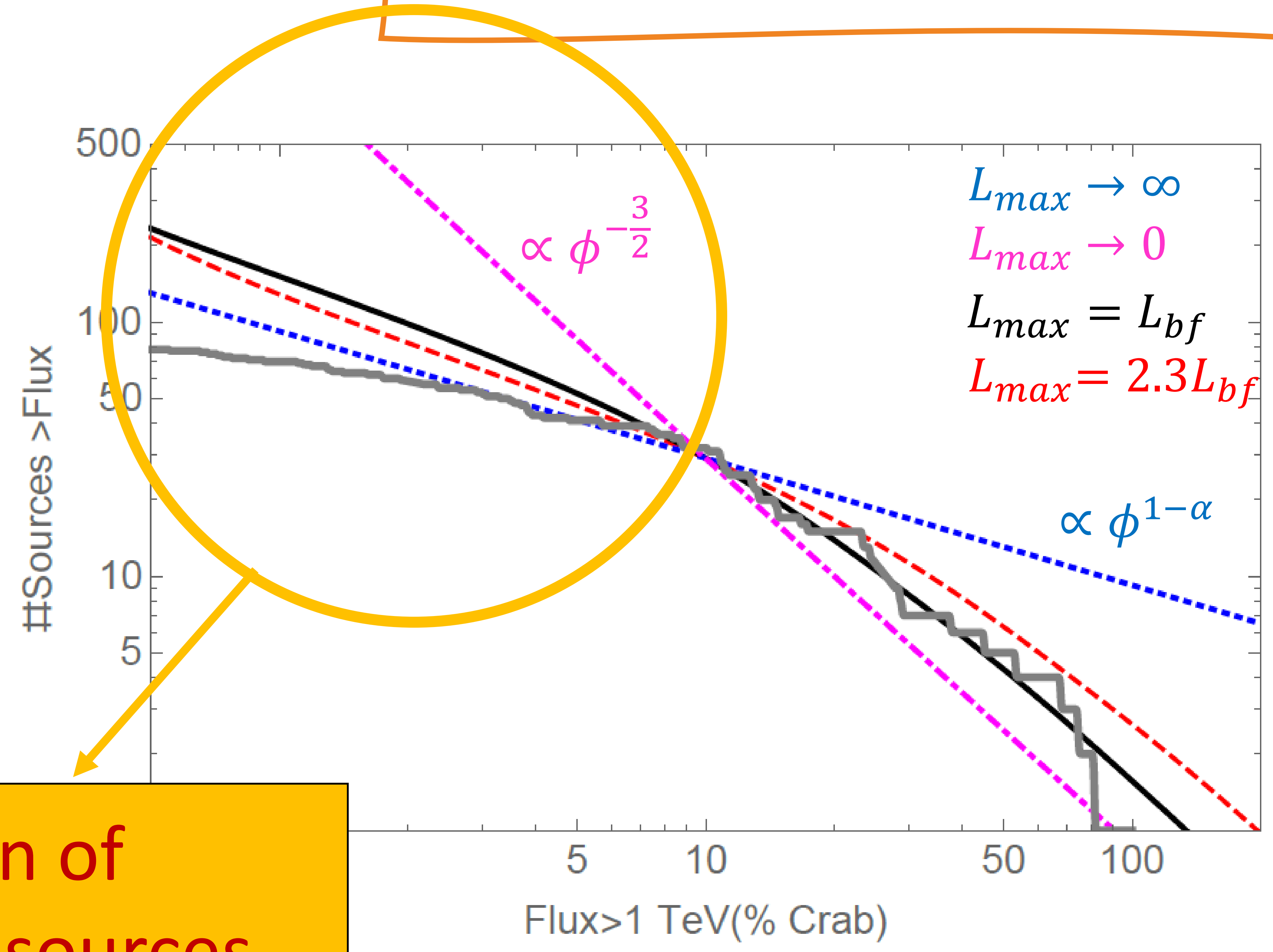

Contribution of unresolved sources

Results:

- The total TeV luminosity (1-100 TeV) of the Galaxy:

$$L_{MW} = \frac{N\, L_{max}}{(2-\alpha)}\left[1 - \left(\frac{L_{min}}{L_{max}}\right)^{\alpha-2}\right] = 1.7^{+0.5}_{-0.4} \times 10^{37}\ erg\ s^{-1}$$

0

- The flux at Earth produced by all sources (1-100 TeV) (resolved and unresolved) in the H.E.S.S. OW:

$$\phi_{tot} = \frac{L_{MW}}{4\Pi\langle E\rangle}\int_{OW} d^3r\, \rho(r) r^{-2} = 3.8^{+1.0}_{-1.0} \times 10^{-10} cm^{-2} s^{-1}$$

3.25 TeV

- By subtraction we can obtain the contribution of unresolved sources in the H.E.S.S. observational window knowing that: $\phi_{S,res} = 2.3 \times 10^{-10} cm^{-2} s^{-1}$ (cumulative flux due to all 78 sources):

$$\phi_{S,unres} = \phi_{tot} - \phi_{S,res} = 1.4^{+1.0}_{-0.8} \times 10^{-10}\ cm^{-2} s^{-1}$$ $\sim 60\%\ \phi_{S,res}$

GSSI

Robustness of the results:

	$\log_{10}\frac{L_{max}}{\mathrm{erg\,s^{-1}}}$	$\mathcal{N}$	$\log_{10}\frac{L_{MW}}{\mathrm{erg\ s^{-1}}}$	Φ_{tot}	τ	$\Delta\chi^2$
Ref.	$35.69^{+0.21}_{-0.28}$	17^{+14}_{-6}	$37.22^{+0.12}_{-0.13}$	$3.8^{+1.0}_{-1.0}$	$1.8^{+1.5}_{-0.6}$	–
SNR	$35.69^{+0.22}_{-0.25}$	18^{+15}_{-7}	$37.23^{+0.12}_{-0.13}$	$3.8^{+1.0}_{-1.0}$	$1.8^{+1.6}_{-0.7}$	1.4
$H = 0.1$ kpc	$35.65^{+0.22}_{-0.27}$	$15^{+14.5}_{-6}$	$37.13^{+0.12}_{-0.13}$	$5.0^{+0.4}_{-2.0}$	$1.6^{+1.5}_{-0.6}$	-7.3
$H = 0.05$ kpc	$35.34^{+0.26}_{-0.19}$	28^{+19}_{-13}	$37.08^{+0.12}_{-0.13}$	$4.4^{+1.3}_{-0.9}$	$2.9^{+2.0}_{-1.4}$	-10.5
$d = 20$ pc	$35.69^{+0.20}_{-0.26}$	17^{+16}_{-6}	$37.23^{+0.12}_{-0.13}$	$3.9^{+0.8}_{-1.0}$	$1.9^{+1.9}_{-0.7}$	-0.2
$d = 40$ pc	$35.67^{+0.20}_{-0.25}$	20^{+20}_{-8}	$37.28^{+0.12}_{-0.13}$	$4.4^{+1.2}_{-1.1}$	$2.2^{+2.0}_{-0.8}$	-1.8
$\alpha = 1.3$	$35.61^{+0.18}_{-0.27}$	$25^{+24}_{-8.5}$	$37.17^{+0.12}_{-0.13}$	$3.5^{+1.1}_{-0.9}$	$4.3^{+4.3}_{-1.5}$	0.0
$\alpha = 1.8$	$35.83^{+0.29}_{-0.24}$	7^{+6}_{-4}	$37.39^{+0.11}_{-0.13}$	$5.9^{+1.8}_{-0.1}$	$0.5^{+0.4}_{-0.2}$	0.5

GS
SI

Robustness of the results:

	$\log_{10}\frac{L_{\max}}{\mathrm{erg\,s^{-1}}}$	$\mathcal{N}$	$\log_{10}\frac{L_{\mathrm{MW}}}{\mathrm{erg\ s^{-1}}}$	Φ_{tot}	τ	$\Delta\chi^2$
Ref.	$35.69^{+0.21}_{-0.28}$	17^{+14}_{-6}	$37.22^{+0.12}_{-0.13}$	$3.8^{+1.0}_{-1.0}$	$1.8^{+1.5}_{-0.6}$	–
SNR	$35.69^{+0.22}_{-0.25}$	18^{+15}_{-7}	$37.23^{+0.12}_{-0.13}$	$3.8^{+1.0}_{-1.0}$	$1.8^{+1.6}_{-0.7}$	1.4
$H=0.1$ kpc	$35.65^{+0.22}_{-0.27}$	$15^{+14.5}_{-6}$	$37.13^{+0.12}_{-0.13}$	$5.0^{+0.4}_{-2.0}$	$1.6^{+1.5}_{-0.6}$	-7.3
$H=0.05$ kpc	$35.34^{+0.26}_{-0.19}$	28^{+19}_{-13}	$37.08^{+0.12}_{-0.13}$	$4.4^{+1.3}_{-0.9}$	$2.9^{+2.0}_{-1.4}$	-10.5
$d=20$ pc	$35.69^{+0.20}_{-0.26}$	17^{+16}_{-6}	$37.23^{+0.12}_{-0.13}$	$3.9^{+0.8}_{-1.0}$	$1.9^{+1.9}_{-0.7}$	-0.2
$d=40$ pc	$35.67^{+0.20}_{-0.25}$	20^{+20}_{-8}	$37.28^{+0.12}_{-0.13}$	$4.4^{+1.2}_{-1.1}$	$2.2^{+2.0}_{-0.8}$	-1.8
$\alpha=1.3$	$35.61^{+0.18}_{-0.27}$	$25^{+24}_{-8.5}$	$37.17^{+0.12}_{-0.13}$	$3.5^{+1.1}_{-0.9}$	$4.3^{+4.3}_{-1.5}$	0.0
$\alpha=1.8$	$35.83^{+0.29}_{-0.24}$	7^{+6}_{-4}	$37.39^{+0.11}_{-0.13}$	$5.9^{+1.8}_{-0.1}$	$0.5^{+0.4}_{-0.2}$	0.5

The quality of the fit improves by reducing the thickness of the disk.

Robustness of the results:

	$\log_{10}\frac{L_{max}}{\mathrm{erg\,s^{-1}}}$	$\mathcal{N}$	$\log_{10}\frac{L_{MW}}{\mathrm{erg\ s^{-1}}}$	Φ_{tot}	τ	$\Delta\chi^2$
Ref.	$35.69^{+0.21}_{-0.28}$	17^{+14}_{-6}	$37.22^{+0.12}_{-0.13}$	$3.8^{+1.0}_{-1.0}$	$1.8^{+1.5}_{-0.6}$	–
SNR	$35.69^{+0.22}_{-0.25}$	18^{+15}_{-7}	$37.23^{+0.12}_{-0.13}$	$3.8^{+1.0}_{-1.0}$	$1.8^{+1.6}_{-0.7}$	1.4
$H = 0.1$ kpc	$35.65^{+0.22}_{-0.27}$	$15^{+14.5}_{-6}$	$37.13^{+0.12}_{-0.13}$	$5.0^{+0.4}_{-2.0}$	$1.6^{+1.5}_{-0.6}$	−7.3
$H = 0.05$ kpc	$35.34^{+0.26}_{-0.19}$	28^{+19}_{-13}	$37.08^{+0.12}_{-0.13}$	$4.4^{+1.3}_{-0.9}$	$2.9^{+2.0}_{-1.4}$	−10.5
$d = 20$ pc	$35.69^{+0.20}_{-0.26}$	17^{+16}_{-6}	$37.23^{+0.12}_{-0.13}$	$3.9^{+0.8}_{-1.0}$	$1.9^{+1.9}_{-0.7}$	−0.2
$d = 40$ pc	$35.67^{+0.20}_{-0.25}$	20^{+20}_{-8}	$37.28^{+0.12}_{-0.13}$	$4.4^{+1.2}_{-1.1}$	$2.2^{+2.0}_{-0.8}$	−1.8
$\alpha = 1.3$	$35.61^{+0.18}_{-0.27}$	$25^{+24}_{-8.5}$	$37.17^{+0.12}_{-0.13}$	$3.5^{+1.1}_{-0.9}$	$4.3^{+4.3}_{-1.5}$	0.0
$\alpha = 1.8$	$35.83^{+0.29}_{-0.24}$	7^{+6}_{-4}	$37.39^{+0.11}_{-0.13}$	$5.9^{+1.8}_{-0.1}$	$0.5^{+0.4}_{-0.2}$	0.5

$$L_{MW} = (1.2 - 2.5) \times 10^{37}\ erg\ s^{-1}$$

$$\phi_{tot} = (3.5 - 5.9)10^{-10} cm^{-2} s^{-1}$$

GSSI

Fading sources powered by pulsar activity

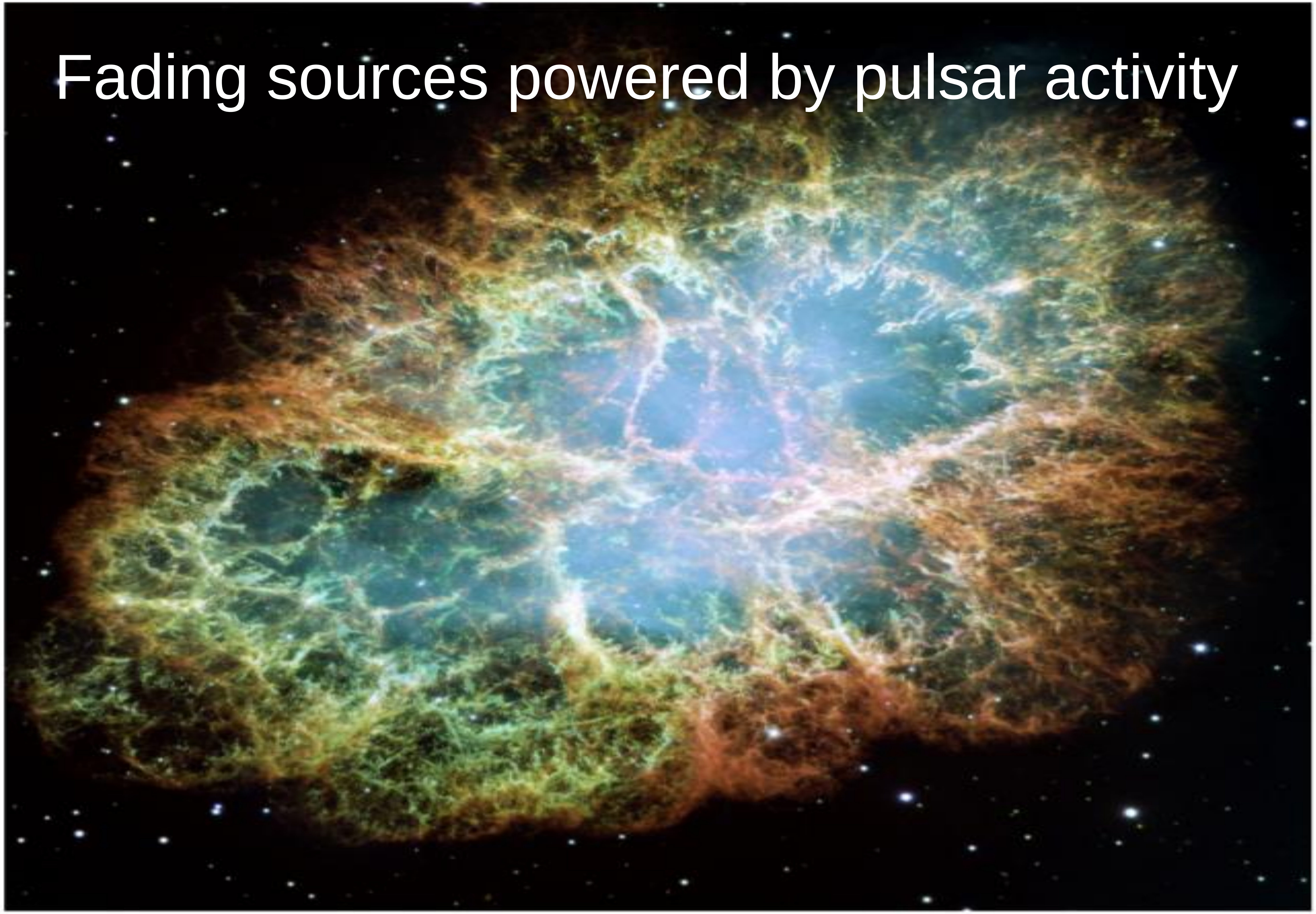

GSSI

Model:

$$\frac{dN}{d^3r\,dL} = \rho(\mathbf{r})\,Y(L)$$

Assuming a fading source population (like PWNe, TeV Halos), the spin-down power is described by:

$$\dot{E}(t) = \dot{E}_0\left(1+\frac{t}{\tau_{sd}}\right)^{-2}$$

Considering that a fraction $\boldsymbol{\lambda(t)}$ of the spin-down power is converted into gamma-rays then the intrinsic luminosity decreases according to:

$\boldsymbol{L_{max}}$

$$L(t) = \lambda(t)\dot{E}(t) = \lambda\dot{E}_0\left(1+\frac{t}{\tau_{sd}}\right)^{-\gamma} \text{ where } \gamma = 2(\delta+1);$$

$$\lambda(t) = \lambda\left(\frac{\dot{E}(t)}{\dot{E}_0}\right)^{\delta}$$

GSSI

Model:

$$\frac{dN}{d^3r\,dL} = \rho(\mathbf{r})\,Y(L)$$

We automatically obtain a power law for the luminosity distribution:

$$Y(L) = \frac{\bar{r}\,\tau\,(\alpha-1)}{L_{\rm max}}\left(\frac{L}{L_{\rm max}}\right)^{-\alpha}$$

Where $\bar{r} = 0.019\ yr^{-1}$ is the SN's rate and $\alpha = \left(\frac{1}{\gamma} + 1\right)$ therefore for $\gamma = 2$ we have $\alpha = 1.5$.

In conclusion the new free parameters are:

- the spin-down timescale τ
- the maximum luminosity of the population L_{max}

GSSI

Model:

The best fit parameters $\boldsymbol{L_{max}}$ and $\boldsymbol{\tau_{sd}}$ are linked to the magnetic field $\boldsymbol{B_0}$ and the initial spin-down period $\boldsymbol{P_0}$ of the pulsar through this relations:

$$L_{max} = \lambda \dot{E}_0 = \lambda \frac{8\pi^4 B_0^2 R^6}{3c^3 P_0^4}$$

$$\tau_{sd} = \frac{3Ic^3 P_0^2}{4\pi^2 B_0^2 R^6}$$

For the firmly identified pulsar from the HGPS catalogue we obtained that the parameter λ is in the range:

$$5 \times 10^{-5} \leq \lambda \leq 5 \times 10^{-2}$$

As a reference value we take $\lambda = 10^{-3}$

$$\frac{\boldsymbol{P_0}}{1\ ms} = 94 \left(\frac{\lambda}{10^{-3}}\right)^{\frac{1}{2}} \left(\frac{\tau}{10^4\ yr}\right)^{-\frac{1}{2}} \left(\frac{L_{max}}{10^{34} erg\ s^{-1}}\right)^{-\frac{1}{2}}$$

$$\frac{\boldsymbol{B_0}}{10^{12} G} = 5.2 \left(\frac{\lambda}{10^{-3}}\right)^{\frac{1}{2}} \left(\frac{\tau}{10^4\ yr}\right)^{-\frac{1}{2}} \left(\frac{L_{max}}{10^{34} erg\ s^{-1}}\right)^{-\frac{1}{2}}$$

Results:

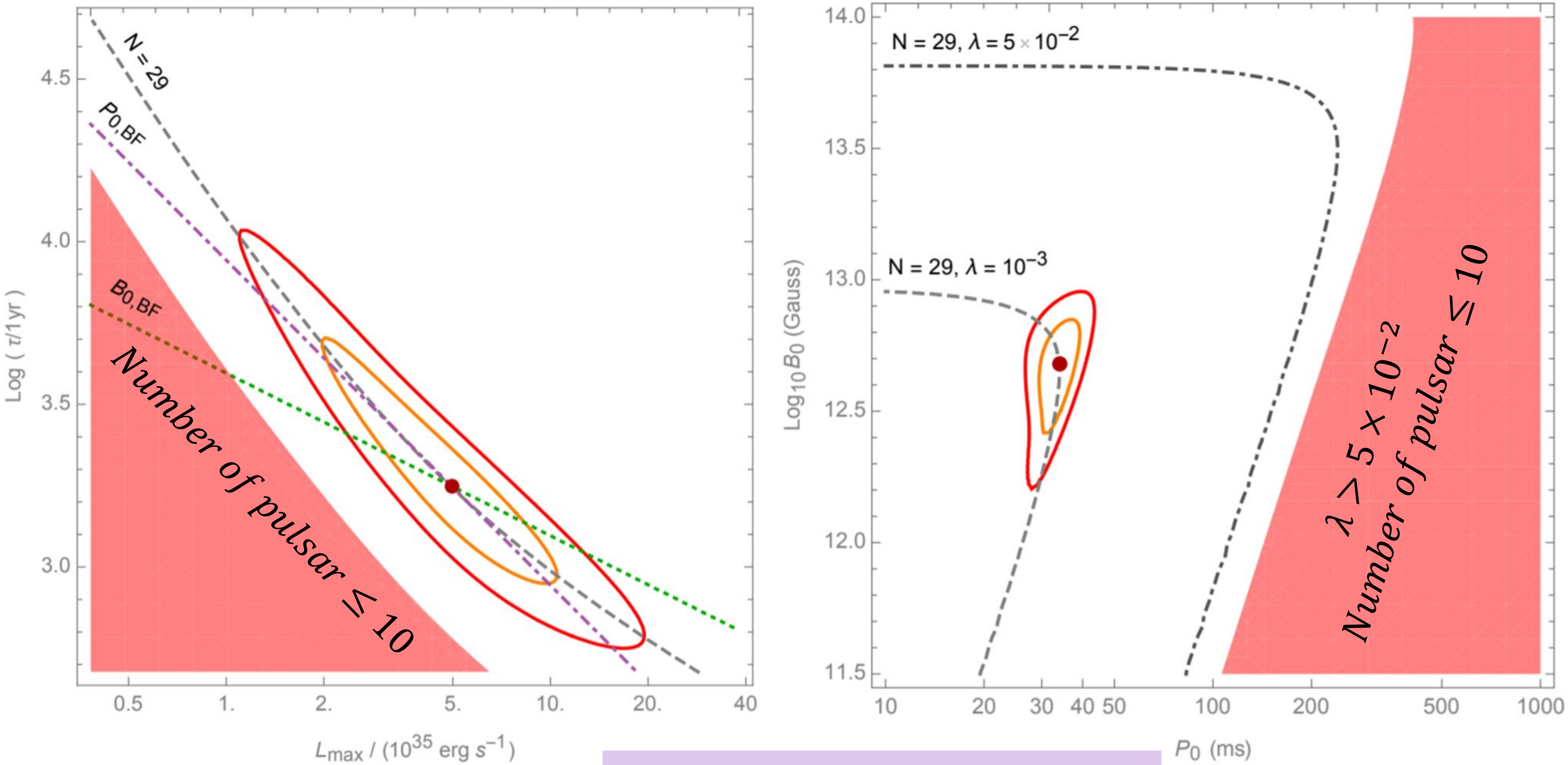

$$\tau_{sd} = 1.8^{+1.5}_{-0.6} \times 10^3 yr$$
$$L_{max} = 4.9^{+3.0}_{-2.1} \times 10^{35} ergs\ s^{-1}$$

$$P_0 = 33^{+5.4}_{-4.3}\ ms \times \left(\frac{\lambda}{10^{-3}}\right)^{\frac{1}{2}}$$

$$B_0 = 4.32(1 \pm 0.45)10^{12} G \times \left(\frac{\lambda}{10^{-3}}\right)^{\frac{1}{2}}$$

G S S I

Conclusions:

- Using the H.G.P.S. we are able to calculate the total Milky Way luminosity in the energy range 1 -100 TeV and the total flux in the H.E.S.S. observational window in the energy range 1 -100 TeV;

- The contribution of unresolved sources is not negligible being $\sim 60\ \%$ of the resolved signal measured by H.E.S.S.;

- In the hypothesis of a fading-source population powered by pulsar activity we are able to predict the general parameters of the pulsar P_0 and B_0. Our predictions are in agreement with values obtained from TeV pulsars but the period is 1 order of magnitude lower than the value observed for radio pulsars.

GS
SI

Future Plans:

- Study of the contribution of unresolved sources for present (Milagro, FermiLAT) and future experiments (CTA);

- Implication of unresolved contribution for the determination of the diffuse component due to cosmic ray interactions.

Thank you for the attention!

Why H.E.S.S?

The fraction of sources of the considered population which are included respectively in the H.E.S.S. ($-110^\circ < l < 60^\circ$ and $|b| < 3^\circ$) and H.A.W.C. ($0^\circ < l < 180^\circ$ and $|b| < 2^\circ$) observation window:

H.E.S.S $\int d^3r\, \rho(\boldsymbol{r}) = 0.816$

H.A.W.C $\int d^3r\, \rho(\boldsymbol{r}) = 0.389$

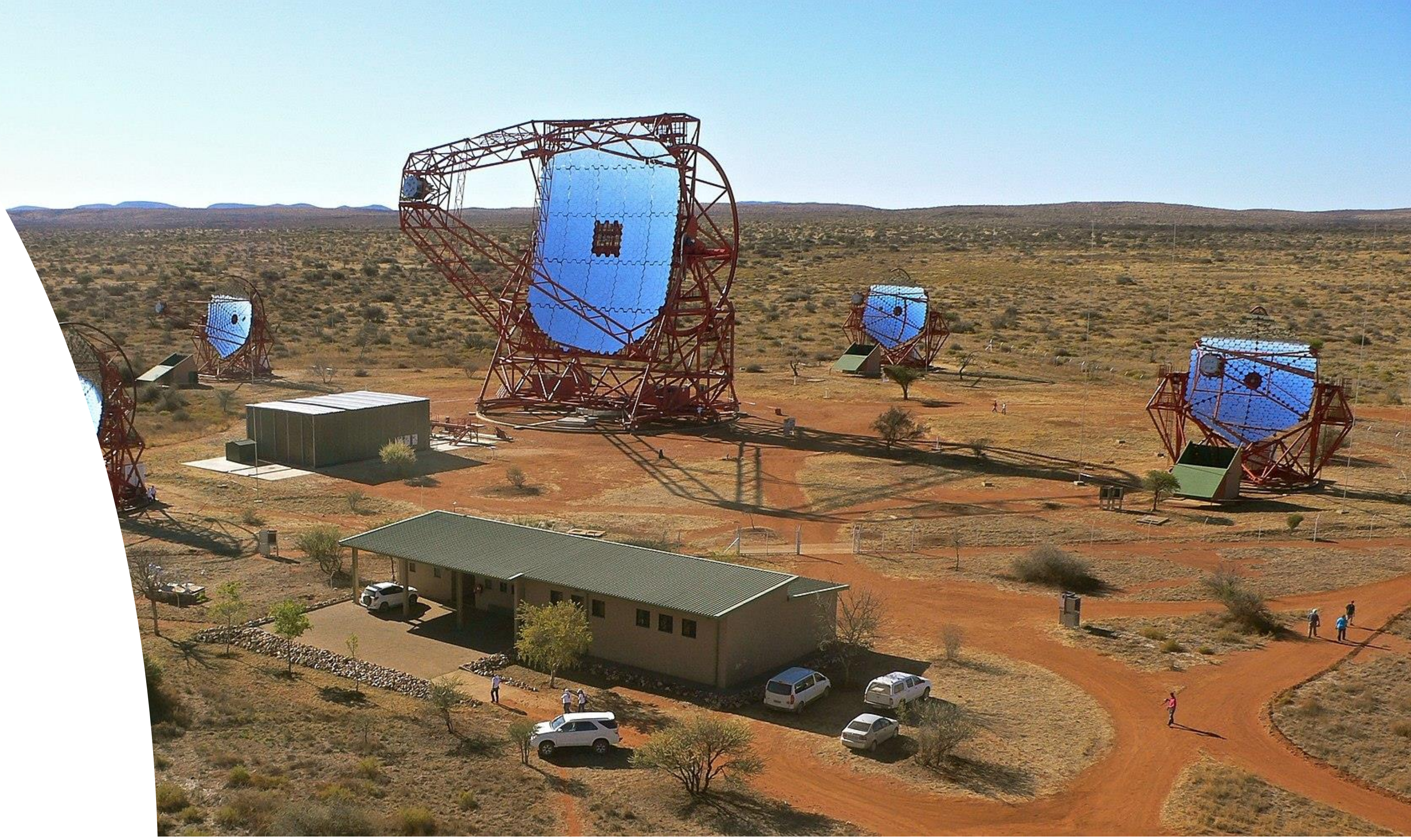

The HAWC Observatory (J. Goodman, Nov. 2016)

H.E.S.S. sensitivity:

- For $0.01\phi_{Crab} \leq \phi \leq 0.1\phi_{Crab}$ the H.E.S.S. sensitivity depends on the angular size of the sources.

- For $\phi \geq 0.1\phi_{Crab}$ all the sources are resolved independently of their angular size. Above this threshold the catalogue is complete.

H.E.S.S. Collaboration: The H.E.S.S. Galactic plane survey

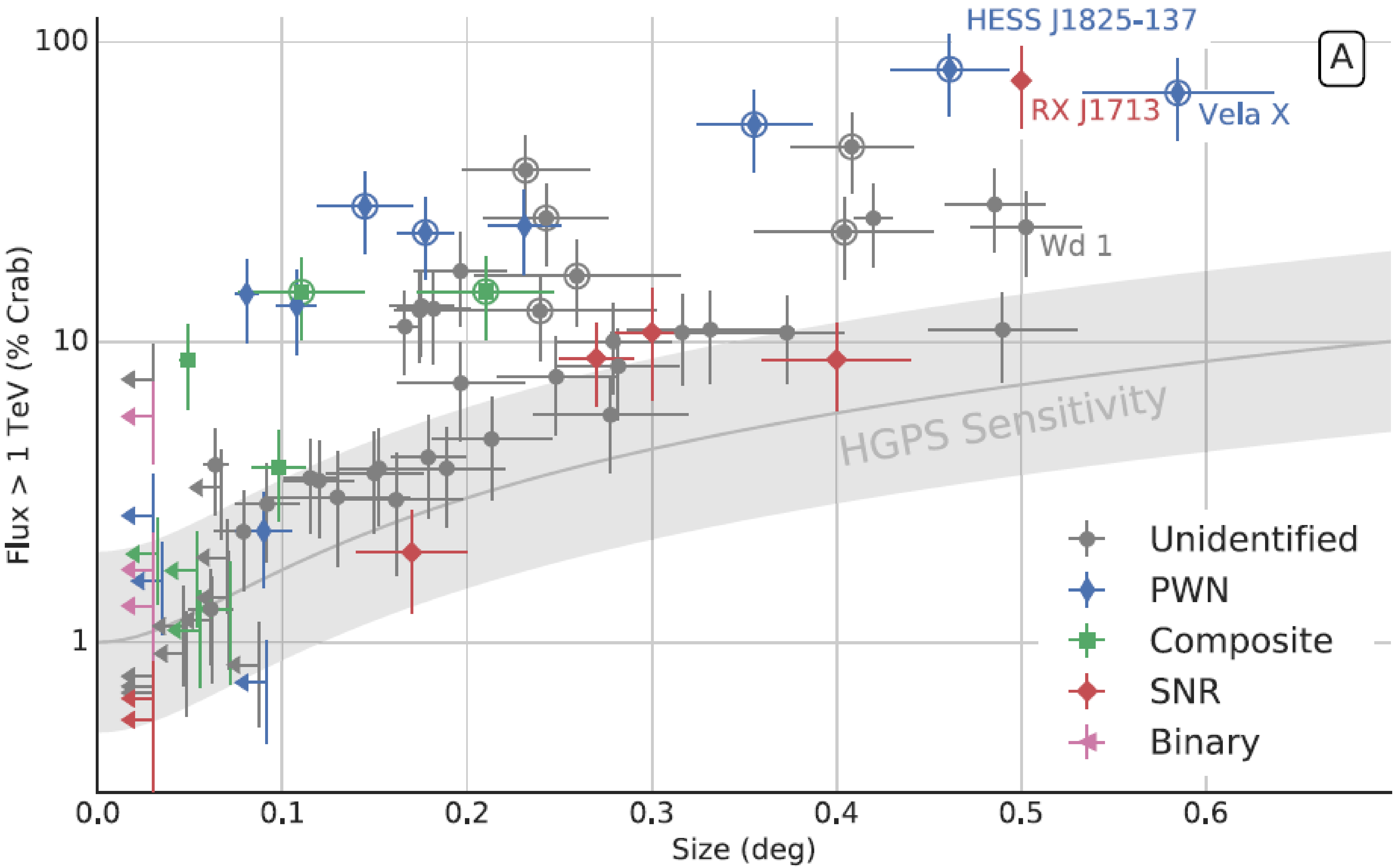

Cumulative distribution:

The flux distribution can be calculated as:

$$\frac{dN}{d\Phi} = \int dr\ 4\pi r^4 \langle E \rangle\ Y(4\pi r^2 \langle E \rangle \Phi)\ \overline{\rho}(r)$$

- $\bar{\rho}(r)$ is the sources spatial distribution integrated over the longitude and latitude intervals probed by H.E.S.S.;
- The above integral is performed in the range $\mathrm{d}/\theta_{max} \leq \mathrm{r} \leq D(L,\phi)$ = where $\theta_{max} = 0.7^{\mathrm{o}}$ is the maximal angular dimension that can be probed by H.E.S.S. and the d is the physical dimention of the source. While $D(L,\phi) = (L/4\,\pi\,\langle E \rangle\,\phi)^{\frac{1}{2}}$;
- We calculate analytically the flux distribution for the 2 limits cases $L_{max} \to \infty$ and $L_{max} \to 0$:

$$\frac{dN}{d\Phi} = R\,\tau\,(\alpha - 1)\,L_{\max}^{\alpha-1}\,\Phi^{-\alpha} \int_0^{\infty} dr\,(4\pi\langle E \rangle)^{1-\alpha}\,r^{4-2\alpha}\,\overline{\rho}(r)$$

$$\frac{dN}{d\Phi} \simeq (4\pi\langle E \rangle)^{1-\alpha}\,\overline{\rho}(0)\,R\,\tau\,(\alpha - 1)\,L_{\max}^{\alpha-1}\,\Phi^{-\alpha} \int_0^{D(L_{\max},\Phi)} dr\,r^{4-2\alpha} = \overline{\rho}(0)\,R\,\tau \left(\frac{\alpha - 1}{5 - 2\alpha}\right) \left(\frac{L_{\max}}{4\pi\langle E \rangle}\right)^{\frac{3}{2}} \Phi^{-\frac{5}{2}}$$

Effect of dispersion in our Model:

We also consider the effects of dispertion of initial period P_0 and magnetic field B_0 around the references values $\tilde{P}_0$ and $\tilde{B}_0$. This turn into a dispertion in $L_{max}(\mathrm{P_0}, \mathrm{B_0})$ and $\tau(\mathrm{P_0}, \mathrm{B_0})$.
We obtain the following luminosity distribution after integrating on $\mathrm{P_0}$ and B_0 distribution:

$$Y(L) = \frac{R\,\widetilde{\tau}\,(\alpha - 1)}{\widetilde{L}} \left(\frac{L}{\widetilde{L}}\right)^{-\alpha} G\left(\frac{L}{\widetilde{L}}\right)$$

Where $\tilde{L}(\tilde{P}_0, \tilde{B}_0)$ and $\tilde{\tau}(\tilde{P}_0, \tilde{B}_0)$ are the spin down time scale and maximum luminosity for the reference values $\tilde{P}_0$ and $\tilde{B}_0$ and $G(x)$ is:

$$G(x) \equiv \int dp\, h(p)\, p^{6-4\alpha} \int db\, g(b)\, b^{2\alpha-4}\, \theta\left(p^{-4}\, b^2 - x\right)$$

Probability distribution for the initial period and it is assumed to be a gaussian distribution in $Log_{10}(p)$ where $p = P/\tilde{P}_0$

Probability distribution for the magnetic field and it is assumed to be a gaussian distribution in $Log_{10}(b)$ where $b = B_0/\tilde{B}_0$

GSSI

Results:

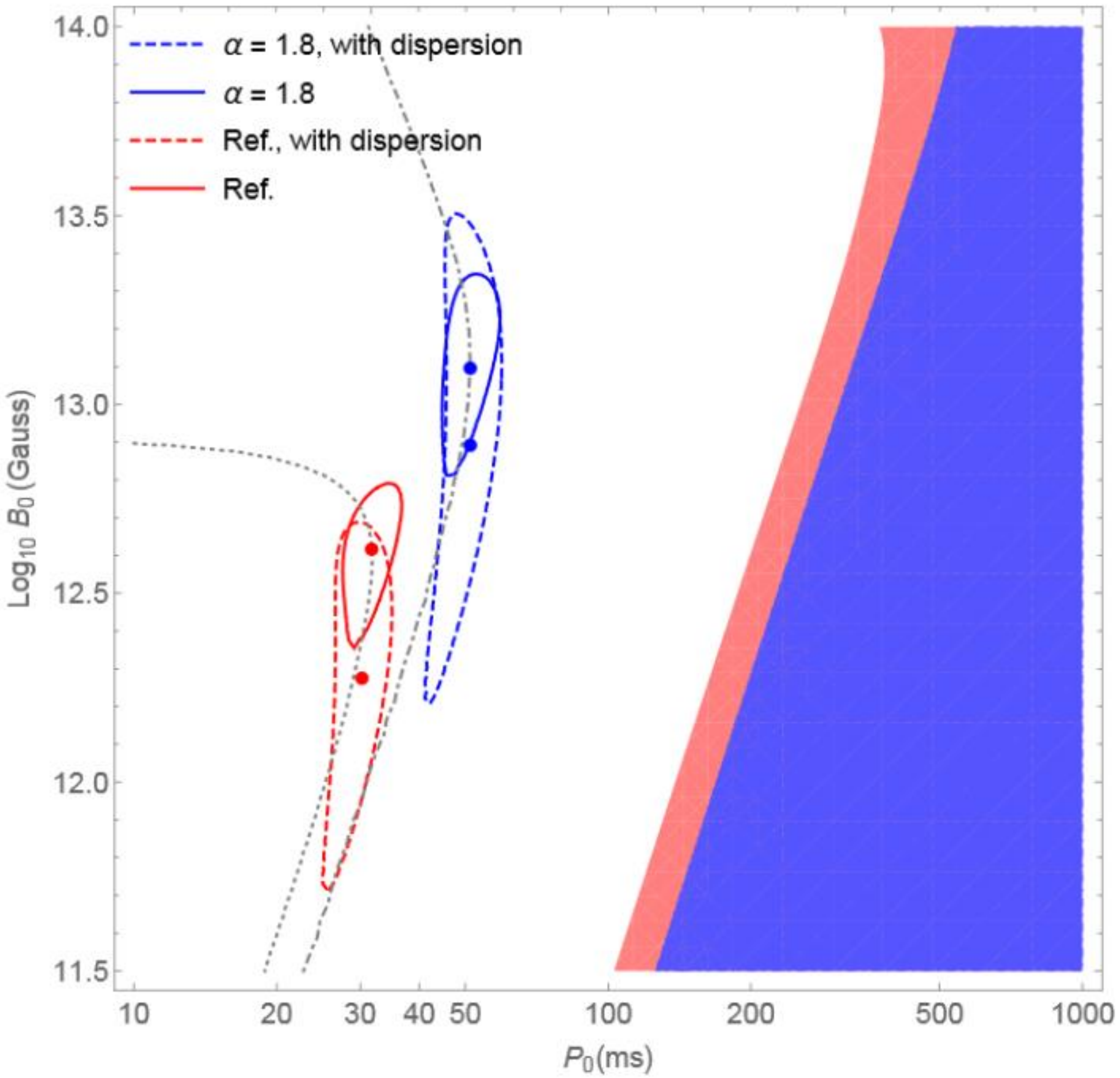

The best fit value of P_0 does not change, while B_0 is slightly reduced as a consequence of the high-luminosity tail of the new source luminosity.

$\alpha = 1.8$

$$B_0 = 12.7^{+9.6}_{-5.8} 10^{12} G \times \left(\frac{\lambda}{10^{-3}}\right)^{\frac{1}{2}}$$

$$P_0 = 51^{+8.1}_{-6.4}\, ms \times \left(\frac{\lambda}{10^{-3}}\right)^{\frac{1}{2}}$$

GS
SI

Milagro excess:

The total flux measured by Milagro at 15 TeV is consisten (whithin uncertainties) with the total flux produced by the HGPS source population in the same observation window ($-\mathbf{30}^{\circ} < \boldsymbol{l} < \mathbf{65}^{\circ}$ and $|\boldsymbol{b}| < \mathbf{2}^{\circ}$):

$$\frac{d\phi_{Milagro}}{dE} \sim 2.9 \times 10^{-12} cm^{-2} s^{-1} sr^{-1} TeV^{-1}$$

$$\frac{d\phi_{HGPS}}{dE} \sim 3.6^{+1.1}_{-0.9} \times 10^{-12} cm^{-2} s^{-1} sr^{-1} TeV^{-1}$$

GSSI

TeV Halo

Stage 1 : The PWN is contained inside the SNR and before the reverse shock (RS) interacts with it. The electrons that are responsible for the TeV gamma-ray emission of the nebula are thought to be confined within the nebula at this stage

Green line : The SNR forward shock (FS) and contact discontinuity (CD)

Stage 2 : The PWN is disrupted by the reverse shock, but before the pulsar escapes its SNR. At this stage, TeV gamma-ray emitting electrons start to escape from the PWN, into the SNR and possibly into the ISM.

Stage 3 : The pulsar has escaped from its —now fading— parent SNR. At this stage, high-energy electrons escape into the surrounding ISM, and may, only then, form a halo.

Sketch of the main evolutionary stages of a PWN

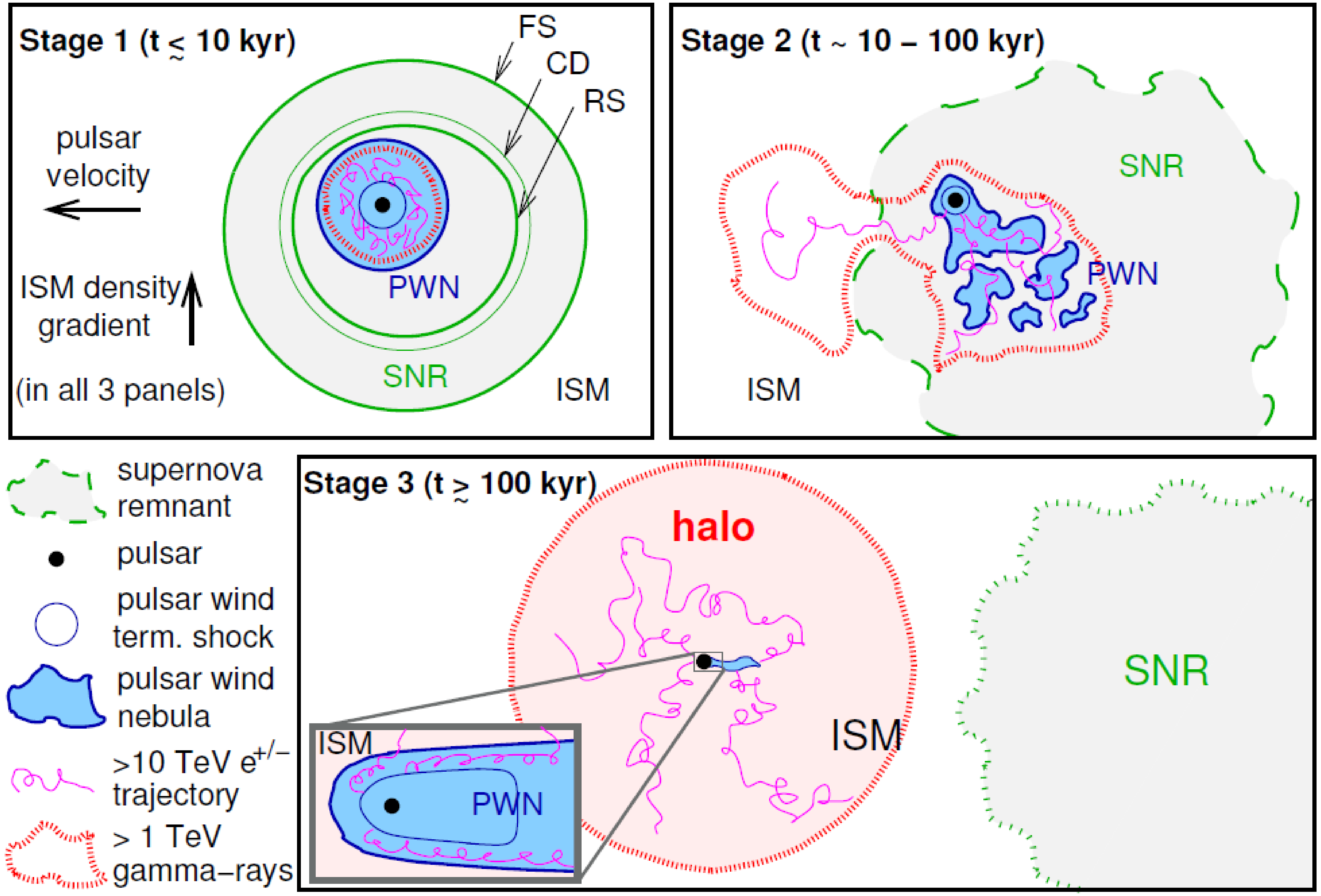

[arXiv:1907.12121v1 [astro-ph.HE] 28 Jul 2019](https://arxiv.org/abs/1907.12121v1)